Identification of *N*-Acylphosphatidylserine Molecules in Eukaryotic Cells†

Ziqiang Guan,‡ Shengrong Li,§ Dale C. Smith,§ Walter A. Shaw,§ and Christian R. H. Raetz*,‡

Department of Biochemistry, Duke University Medical Center, P.O. Box 3711, Durham, North Carolina 27710, and Avanti Polar Lipids, Inc., 700 Industrial Park Drive, Alabaster, Alabama 35007

Received September 18, 2007; Revised Manuscript Received October 16, 2007

ABSTRACT: While profiling the lipidome of the mouse brain by mass spectrometry, we discovered a novel family of *N*-acylphosphatidylserine (*N*-acyl-PS) molecules. These *N*-acyl-PS species were enriched by DEAE-cellulose column chromatography, and they were then characterized by accurate mass measurements, tandem mass spectrometry, liquid chromatography/mass spectrometry, and comparison to an authentic standard. Mouse brain *N*-acyl-PS molecules are heterogeneous and constitute about 0.1% of the total lipid. In addition to various ester-linked fatty acyl chains on their glycerol backbones, the complexity of the *N*-acyl-PS series is further increased by the presence of diverse amide-linked *N*-acyl chains, which include saturated, monounsaturated, and polyunsaturated species. *N*-Acyl-PS molecular species were also detected in the lipids of pig brain, mouse RAW264.7 macrophage tumor cells, and yeast, but not *Escherichia coli*. *N*-Acyl-PSs may be biosynthetic precursors of *N*-acylserine molecules, such as the recently reported signaling lipid *N*-arachidonoylserine from bovine brain. We suggest that a phospholipase D might cleave *N*-acyl-PS to generate *N*-acylserine, in analogy to the biosynthesis of the endocannabinoid *N*-arachidonoylethanolamine (anadamide) from *N*-arachidonoylphosphatidylethanolamine.

A comprehensive qualitative and quantitative characterization of lipids in the context of systems biology is crucial to a complete understanding of cellular physiology and pathology and is the rationale behind the Lipid Maps Consortium (www.lipidmaps.org) (*1*, *2*). One of the major aims of the project is to discover novel lipids, with emphasis on those from mouse RAW264.7 macrophage tumor cells. There is ample biochemical and genomic evidence indicating the existence of novel lipids. For instance, radiochemical experiments with high levels of $^{32}P_i$ indicate the presence of numerous unidentified minor phospholipid species at levels of 0.1% or less in the total lipids of both prokaryotic and eukaryotic cells (*3*, *4*). In addition, genomic analyses suggest the existence of proteins of unknown function, distantly related in their primary sequences to well-characterized enzymes of lipid metabolism (*5*). These predicted proteins might be involved in the biosynthesis of some of the minor unknown lipids.

State-of-the-art, high-resolution mass spectrometry (MS)[1] represents a powerful initial approach to the identification and structural characterization of novel lipids. Although MS has long been employed for the characterization of lipid molecules (*6*, *7*), the introduction of electrospray ionization (ESI) (*8*) and matrix-assisted laser desorption ionization (MALDI) (*9*) dramatically improved the applicability of MS for lipid analysis. These two soft ionization techniques, together with instrumentation developments, have allowed intact, labile lipid molecules to be analyzed directly by MS with exceedingly high sensitivity and molecular specificity (*6*, *10*, *11*), including the detection of trace biosynthetic intermediates (*12*).

By combining large-scale phospholipid prefractionation procedures with high-resolution ESI-MS/MS analysis, we have now discovered a family of novel *N*-acylphosphatidylserine (*N*-acyl-PS) molecules in mouse brain, pig brain, mouse RAW264.7 macrophage tumor cells, and yeast. The proposed structures of these *N*-acyl-PS species were confirmed by comparison with a synthetic standard. In 1970, Nelson provided preliminary evidence for the presence of *N*-acyl-PS in sheep red blood cells. However, mass spectrometry and NMR were not used to characterize this material, and no follow-up studies were published. Donahue et al. reported the presence of *N*-acyl-PS as a major component of *Rhodopseudomonas sphaeroides* phospholipids in 1982 (*13*), but Schmid et al. later demonstrated that the proposed *R. sphaeroides N*-acyl-PS was actually phosphatidyl-Tris, arising by phosphatidyl group transfer to the Tris buffer present in the growth medium (*14*). To our knowledge, no subsequent reports of *N*-acyl-PS as a component of biological membranes have appeared. We suggest that *N*-acyl-PS may function as a precursor of *N*-acyl-L-serine in animal cells, a bioactive signaling lipid recently isolated from bovine brain (*15*). The biosynthesis, metabolism, and function of *N*-acyl-PS may be analogous to that of *N*-acylphosphatidylethanolamine (*N*-acyl-PE), the precursor of the mammalian endocannabinoid *N*-arachidonylethanolamine (*16*−*18*). The unequivocal identification of a family of *N*-acyl-PS molecular species in brain, macrophages, and yeast set

† This research was supported by LIPID MAPS Large Scale Collaborative Grant Number GM-069338 from NIH.

* To whom correspondence should be addressed. Phone: (919) 684-3384. Fax: (919) 684-8885. E-mail: raetz@biochem.duke.edu.

‡ Duke University Medical Center.

§ Avanti Polar Lipids, Inc.

[1] Abbreviations: ESI-MS, electrospray ionization mass spectrometry; LC/MS, liquid chromatography/mass spectrometry; MRM, multiple reaction monitoring; MS/MS, tandem mass spectrometry; *N*-acyl-PE, *N*-acylphosphatidylethanolamine; *N*-acyl-PS, *N*-acylphosphatidylserine; NAGPS, *N*-acylglycerophosphoserine; PBS, phosphate-buffered saline.

10.1021/bi701907g CCC: $37.00
Published on Web 11/22/2007

the stage for the complete elucidation of its biosynthesis, turnover, and function.

EXPERIMENTAL PROCEDURES

Materials. Total porcine brain lipids (product number 131101) were obtained from Avanti Polar Lipids, Inc. (Alabaster, AL). The *N*-acyl-PS standard, 1,2-dioleoyl-*sn*-glycerol-3-phospho-*N*-nonadecanoyl-L-serine, was synthesized by reacting 1,2-dioleoyl-*sn*-glycerol-3-phospho-L-serine (product number 840035, Avanti Polar Lipids, Inc.) with the *N*-hydroxysuccinimide ester of nonadecanoic acid in anhydrous dimethylformamide. The crude product was purified by column chromatography on silica gel. The 1,2-dioleoyl-*sn*-glycerol-3-phospho-*N*-nonadecanoyl-L-serine was obtained as a clear oil [^{1}H NMR (δ, $CDCl_3$) 0.89 (m, 9H, 3 × CH_3), 1.25 (m, 70H, 35 × CH_2), 1.59 (s, br, 6H, β-CH_2), 2.16 (s, br, 8H, allylic CH_2), 2.29 (m, 6H, α-CH_2), 3.92 (s, br, 2H, *sn*-3-CH_2), 4.00 (s, br, 1H, CH on serine), 4.12 (dd, J = 6.8 and 11.2 Hz, 1H, *sn*-1-CH_2), 4.35 (d, J = 10.6 Hz, 2H, CH_2 on serine), 4.64 (s, br, 1H, *sn*-1-CH_2), 5.20 (s, br, 1H, *sn*-2-CH), 5.34 (m, 4H, alkenyl CH), 7.12 (s, br, 4H, NH_4^+ counterion); P^{31} NMR (δ, $CDCl_3$) 0.11 (s, br)]. Chemicals, HPLC-grade solvents, Dounce tissue grinders (Potter−Elvehjem style), and Whatman DE-23 DEAE-cellulose anion-exchange resin were purchased from VWR (West Chester, PA). Mouse brains isolated from 18 month old E3/3 mice were provided by Dr. Patrick Sullivan (Duke University Medical Center).

Extraction and Anion-Exchange Fractionation of Mouse Brain Lipids. Mouse brains were isolated as previously described (*19*). Half of a frozen mouse brain (∼0.5 g) was homogenized in 10 mL of ice-cold chloroform/methanol (1:2, v/v) and 2.5 mL of ice-cold phosphate-buffered saline (PBS) (*20*) using a Dounce tissue grinder. The homogenate was then transferred to a glass tube with a Teflon-lined cap, vigorously mixed by using a vortex for about 2 min, and then incubated on ice for 10 min. Following centrifugation at 3000*g* at 4 °C for 10 min, the supernatant was transferred to a new glass tube, while the insoluble debris was discarded. The supernatant was then converted to a two-phase Bligh/Dyer system (*21*) by adding 3.3 mL of chloroform and 3 mL of PBS. After vigorous mixing, the phases were separated by centrifugation at 3000*g* at 4 °C for 10 min, and the lower phase was dried under a stream of nitrogen. The anion-exchange fractionation of mouse brain total lipids was performed as previously described (*22*, *23*). Briefly, the dried mouse brain lipids were redissolved in 2 mL of chloroform/methanol/water (2:3:1, v/v/v) and applied to a 1 mL DEAE-cellulose column (acetate form) equilibrated with the same solvent mixture (*22*, *23*). Following sample loading, the column was washed with 5 mL of chloroform/methanol/water (2:3:1, v/v/v). The bound lipids were eluted stepwise with 5 mL washes of chloroform/methanol/aqueous ammonium acetate (2:3:1, v/v/v), with increasing ammonium acetate concentrations of 30, 60, 120, 240, and 480 mM as the aqueous component. All fractions were converted to a two-phase Bligh/Dyer system by adding appropriate volumes of chloroform and water. The lower phases were dried under a stream of nitrogen and stored at −20 °C until MS analysis.

High-Resolution Electrospray Ionization/Mass Spectrometry. High-resolution ESI mass spectra were acquired on a QSTAR XL quadrupole time-of-flight tandem mass spectrometer (Applied Biosystems, Foster City, CA) equipped with an electrospray source. For ESI-MS analysis, the entire 120 mM fraction from DEAE anion exchange of mouse brain lipids (prepared as described above) was redissolved in 200 μL of chloroform/methanol (2:1, v/v). Typically, 10 μL of this solution was diluted into 200 μL of chloroform/methanol (1:1, v/v) and then infused into the ESI source at 5−10 μL/min. The negative and positive electrospray voltages were set at −4200 and +5500 V, respectively. Other MS settings were as follows: CUR = 20 psi (pressure), GS1 = 20 psi, DP = −55 V, and FP = −265 V. For MS/MS, collision-induced dissociation was performed with collision energy ranging from 40 to 70 V (laboratory frame of energy) and with nitrogen as the collision gas. Data acquisition and analysis were performed using the Analyst QS software.

Liquid Chromatography/Mass Spectrometry. LC/MS of lipids was performed using a Shimadzu LC system (comprising a solvent degasser, two LC-10A pumps, and an SCL-10A system controller) coupled to a QSTAR XL quadrupole time-of-flight tandem mass spectrometer (as above). LC was performed at a flow rate of 200 μL/min with a linear gradient as follows: 100% mobile phase A was held isocratically for 2 min and then linearly increased to 100% mobile phase B over 14 min and held at 100% B for 4 min. Mobile phase A consisted of methanol/acetonitrile/aqueous 1 mM ammonium acetate (60:20:20, v/v/v). Mobile phase B consisted of 100% ethanol containing 1 mM ammonium acetate. A Zorbax SB-C8 reversed-phase column (5 μm, 2.1 × 50 mm) was obtained from Agilent (Palo Alto, CA). The postcolumn splitter diverted ∼10% of the LC flow to the ESI source of the mass spectrometer.

Anion-Exchange Fractionation of Porcine Brain Total Lipids and Mild Alkaline Hydrolysis of N-Acyl-PS. The anion-exchange fractionation of porcine brain total lipids from Avanti Polar Lipids (part number 131101) was carried out on an Agilent 1200 HPLC system. The DEAE column (DEAE-5PW, 10 μm, 7.5 mm × 7.5 cm) was from Sigma. The LC flow rate was 2 mL/min. Solvent A consisted of chloroform/methanol/water (2:3:1, v/v/v). Solvent B consisted of chloroform/methanol/480 mM ammonium acetate (2:3:1, v/v/v). Lipid fractionation was carried out by step elution: after 100 mg of porcine brain total lipids in 1.5 mL of chloroform/methanol/water (2:3:1, v/v/v) was loaded onto the DEAE column, the lipids were eluted with 16 mL steps of chloroform/methanol/aqueous ammonium acetate (2:3:1, v/v), with ammonium acetate concentrations of 0, 30, 60, 120, 240, and 480 mM successively in the aqueous component. Each fraction was then converted to a two-phase Bligh/Dyer system consisting of chloroform/methanol/water (2:2:1.8, v/v/v) by adding appropriate volumes of chloroform and water. The lower phases were dried under a stream of nitrogen. The 120 mM fraction, containing the *N*-acyl-PS, was subjected to mild alkaline hydrolysis in a 3.8 mL mixture of $CHCl_3$/MeOH/0.38 N NaOH (1:2:0.8, v/v) at room temperature (24 °C) for 1 h. Following hydrolysis, the reaction mixture was neutralized by adding concentrated HCl (37%) using a glass micropipet, as judged by pH paper. The system was converted to a two-phase Bligh/Dyer mixture consisting of chloroform/methanol/water (2:2:1.8, v/v/v) by adding appropriate volumes of chloroform and water. Following centrifugation at ∼500*g* at room temperature for 10

min using a clinical centrifuge, the lower phase was dried under a stream of nitrogen and stored at −20 °C. For LC/MS analysis, the dried hydrolysis products were redissolved in 100 μL of MeOH/DMSO (1:1, v/v), 10 μL of which was injected onto a C8 column for LC/MS using the QSTAR XL mass spectrometer as described above.

Analysis of the Level of Brain N-Acyl-PS by Liquid Chromatography−Multiple Reaction Monitoring. The level of *N*-acyl-PS in total porcine brain lipids was estimated by the method of multiple reaction monitoring (MRM) on a 4000 Q-Trap hybrid triple-quadrupole linear ion trap mass spectrometer equipped with a Turbo V ion source (Applied Biosystems). LC−MRM analysis was performed in the negative ion mode with MS settings as follows: CUR = 20 psi (pressure), GS1 = 20 psi, GS2 = 30 psi, IS = −4500 V, TEM = 350 °C, ihe = ON, DP = −70 V, EP = −10 V, and CXP = −5 V. The voltage used for collision-induced dissociation was −50 V. To estimate the level of brain *N*-acyl-PS, a known quantity of synthetic *N*-acyl-PS standard (Avanti) was added to a defined amount of the total porcine brain lipids dissolved in 1 mL of MeOH/DMSO (1:1, v/v), with final concentrations of 0.1 ng/μL for the synthetic *N*-acyl-PS and 0.1 μg/μL for the porcine brain total lipid. A 10 μL portion of the sample solution was then injected onto a C8 column for each LC−MRM analysis, with the LC conditions as described above, but without flow splitting.

Extraction and Anion-Exchange Fractionation of Lipids from RAW264.7 Cells. Five 150 mm plates of RAW 264.7 cells were cultured as previously described (*24*) and were extracted using the method of Bligh and Dyer (*21*). Each plate of RAW cells at about 90% confluence was washed with 10 mL of PBS and then scraped into 5 mL of PBS (137 mM NaCl, 0.027 mM KCl, 0.01 mM Na_2HPO_4, and 0.0018 mM KH_2PO_4) (*20*). The cell suspension was centrifuged at 4000*g* to harvest the cells. The cell pellets from five plates were combined, resuspended in 4 mL of PBS, and then transferred in equal volumes (2 mL) to two glass tubes equipped with Teflon-lined caps. To each tube were added 2.5 mL of chloroform and 5 mL of methanol to form a single-phase Bligh/Dyer system. The contents were vigorously mixed on a vortex and then subjected to sonic irradiation in a bath apparatus for 2 min. Following incubation at room temperature for 15 min, the single-phase Bligh/Dyer mixtures were centrifuged at ∼500*g* for 10 min in a clinical centrifuge to pellet cell debris. Each supernatant was transferred to a fresh tube, followed by addition of 2.5 mL of chloroform and 2.5 mL of PBS to generate two-phase Bligh/Dyer systems. After mixing, the two tubes were centrifuged as above to resolve the phases. The two lower phases were combined, dried under a stream of nitrogen, and stored at −20 °C. The anion-exchange fractionation of lipids from RAW cells on a DEAE-cellulose column and the negative ion ESI-MS analysis were performed as described above (for the mouse brain lipids).

Identification of N-Acyl-PS in Yeast. Frozen cells of *Saccharomyces cerevesiae* BY4743 were provided by Dr. Arnold Greenleaf of the Duke University Medical Center. Lipid extraction of the yeast cells was performed using the method of Bligh and Dyer (*21*). Specifically, about 0.2 g of frozen yeast cell pellet was resuspended in a 3.8 mL mixture of $CHCl_3$/MeOH/PBS (1:2:0.8, v/v) in a glass tube with a Teflon-lined cap, was vigorously mixed on a vortex for 2 min, and was then subjected to sonic irradiation in a bath apparatus for 10 min. Following incubation at room temperature for 15 min, the single-phase Bligh/Dyer mixture was centrifuged at ∼500*g* for 10 min in a clinical centrifuge to pellet cell debris. The supernatant was transferred to a fresh tube, followed by the addition of 1 mL of chloroform and 1 mL of PBS to generate a two-phase Bligh/Dyer system (*21*). After mixing, the tube was centrifuged as above to resolve the phases. The lower phase was dried under a stream of nitrogen and stored at −20 °C. For LC/MS (Q-Star XL) and LC−MRM (4000 Q-Trap) analysis, the dried yeast lipid extract was redissolved in 100 μL of $CHCl_3$. Typically, 10 μL of this solution (in $CHCl_3$) was mixed with 90 μL of DMSO/MeOH (1:1, v/v), and 10 μL of the final solution was injected for each analysis using the LC conditions described above.

RESULTS

Large-Scale Prefractionation of Anionic Mouse Brain Lipids. Eukaryotic lipids can be separated on the basis of their net negative charge by DEAE-cellulose column chromatography in chloroform/methanol/water (2:3:1, v/v). The column capacity is 1−10 mg of lipid/mL of resin, and the process can be scaled from the microgram to the gram range (*22*, *23*, *25*). The zwitterionic lipids (predominantly phosphatidylethanolamines, phosphatidylcholines, and sphingomyelins) and the uncharged lipids (triacylglcyerols, diacylglycerols, ceramides, dolichols, and sterols) emerge in the run-through. These compounds account for about three-quarters of the total brain lipids. They can be further fractionated by normal- or reversed-phase chromatography during LC/MS analysis. The anionic lipids (which include the phosphatidylserines, phosphatidylinositols, cardiolipins, sulfatides, phosphatidylglycerols, and phosphatidic acids) bind to the column. These substances are step-eluted with increasing concentrations (30, 60, 120, 240, and 480 mM) of ammonium acetate as the aqueous component of chloroform/methanol/water (2:3:1, v/v). The singly charged phosphtidylinositols, phosphatidyglycerols, and phosphatidylserines emerge with 30−60 mM ammonium acetate, whereas the more acidic phosphatidic acids, sulfatides, and cardiolipins emerge with 60−120 mM ammonium acetate. Residual cardiolipins and minor acidic lipids, such as CDP−diacylglycerols and the phosphatidylinositol phosphates, emerge with 240−480 mM ammonium acetate. Each fraction contains additional minor lipids, many of which are poorly characterized. Prefractionation of biological lipids prior to analysis by ESI-MS or LC/MS reduces signal suppression of the less abundant ions by the major components.

Identification of N-Acyl-PS Molecular Species. Figure 1A shows the negative ion ESI mass spectrum of mouse brain lipids eluting from DEAE-cellulose with 120 mM ammonium acetate as the aqueous component of chloroform/methanol/water (2:3:1, v/v). The major peaks were identified by MS/MS as the $[M - H]^-$ ions of phosphatidic acids, sulfatides, or residual phosphatidyserines and the $[M - H]^{2-}$ ions of cardiolipins. Several singly charged ions in the range of *m*/*z* 1000−1100 could not readily be assigned to known compounds. Among them, the most abundant was seen at *m*/*z* 1026.78. It was interpreted as $[M - H]^-$, given the presence of a strong putative $[M + H]^+$ ion at *m*/*z* 1028.80 in the positive mode (data not shown). The unknown ion at *m*/*z*

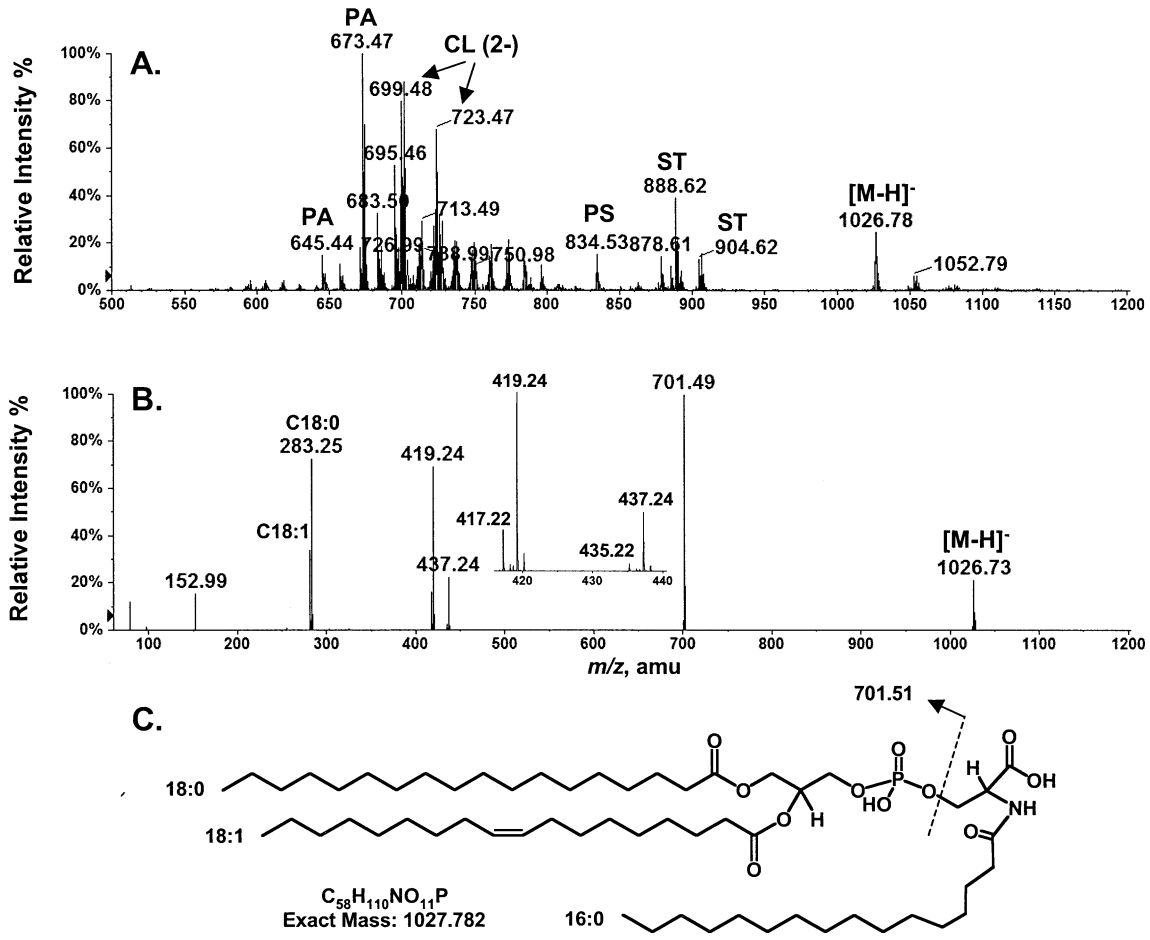

FIGURE 1: Negative ion ESI-MS analysis and proposed structure of a novel brain lipid with $[M - H]^-$ at *m*/*z* 1026.78: (A) negative ion ESI-MS of mouse brain lipids eluting from DEAE-cellulose with 120 mM aqueous ammonium acetate, (B) MS/MS analysis of *m*/*z* 1026.78, (C) proposed brain *N*-acyl-PS structure (1-stearoyl-2-oleoyl-*sn*-glycerol-3-phospho-*N*-palmitoylserine) for the species with $[M - H]^-$ at *m*/*z* 1026.78. Abbreviations: PA, phosphatidic acid; CL, cardiolipin; PS, phosphatidylserine; ST, sulfatide.

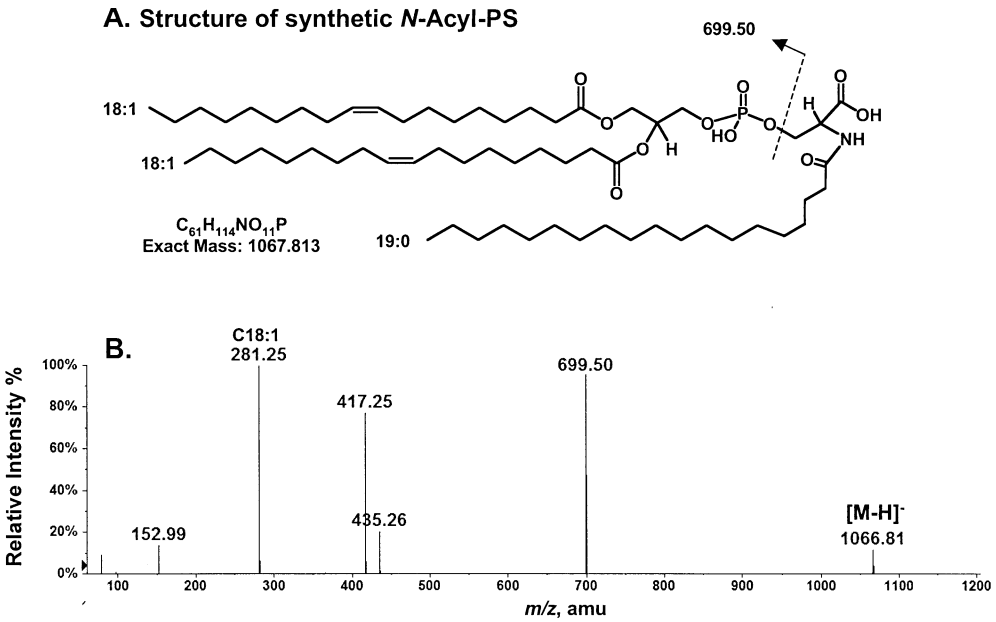

FIGURE 2: Negative ion ESI-MS analysis of synthetic *N*-acyl-PS: (A) structure of the synthetic standard (1,2-dioleoyl-*sn*-glycerol-3-phospho-*N*-nonadecanoylserine), (B) negative ion MS/MS analysis of the synthetic *N*-acyl-PS $[M - H]^-$ ion at *m*/*z* 1066.81.

1026.78 (Figure 1A) was analyzed by MS/MS (Figure 1B), yielding product ions at *m*/*z* 78.96 (PO_3^-), 96.97 ($H_2PO_4^-$), and 152.99 ($C_3H_6O_5P^-$) consistent with a glycerophospholipid. The two acyl chains esterified to the glycerol backbone were identified as stearic (C18:0) and oleic (C18:1) acids, as judged by the prominent ions at *m*/*z* 283.25 and 281.25, respectively. This assignment is furthermore consistent with the signal at *m*/*z* 701.49, which could be a phosphatidic acid

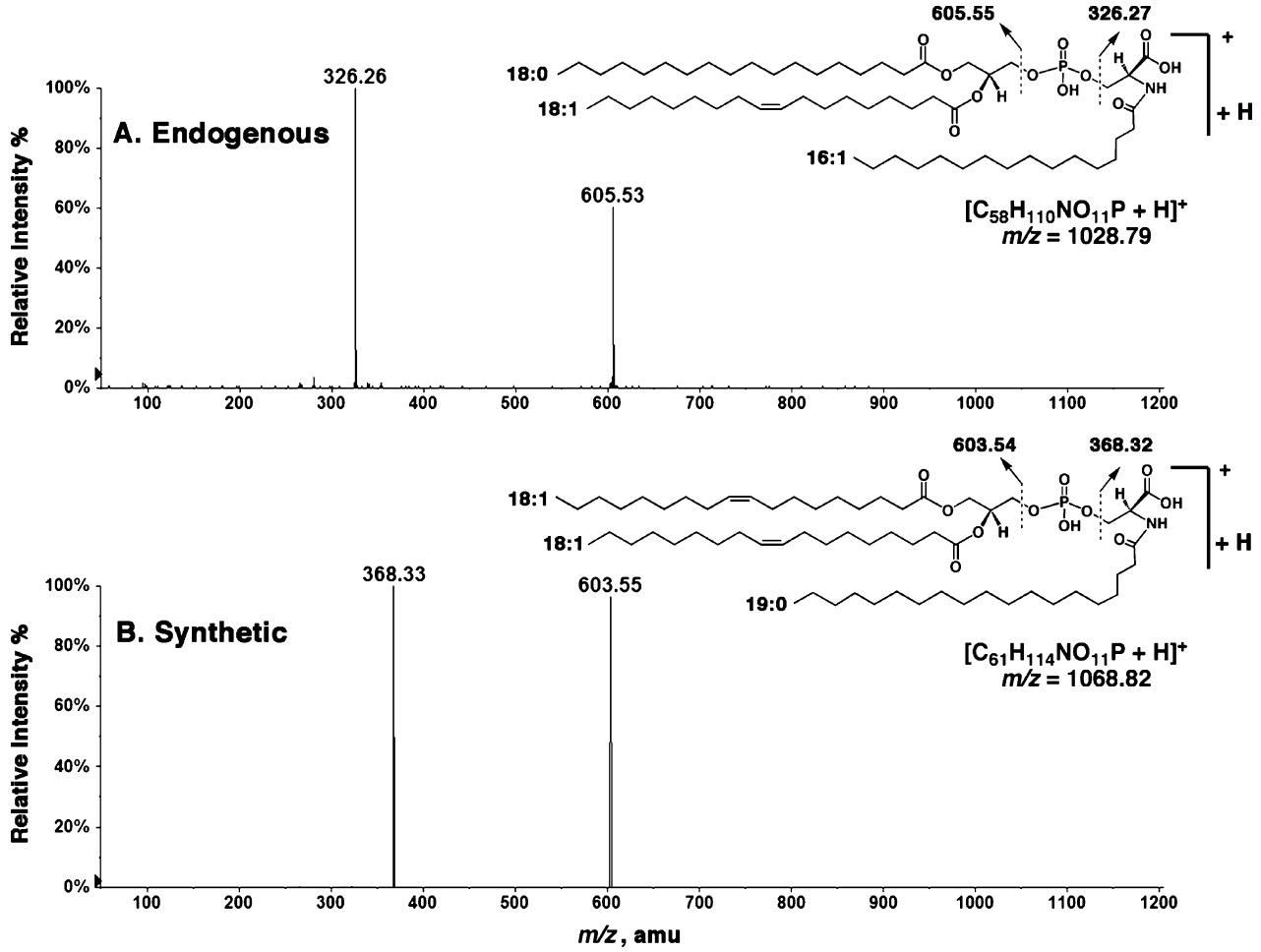

FIGURE 3: Comparison of the endogenous and synthetic *N*-acyl-PS molecules by MS/MS of their $[M + H]^+$ ions: (A) MS/MS spectrum of the $[M + H]^+$ ion at *m/z* 1028.79 (endogenous), (B) MS/MS spectrum of the $[M + H]^+$ ion at *m/z* 1068.82 (synthetic). The major product ions are indicated on the inset structures.

anion esterified with C18:0 and C18:1 on its glycerol backbone. The ions at *m/z* 419.24 and 437.24 would be derived from the phosphatidic acid ion by neutral loss of the C18:1 moiety as a fatty acid (RCO_2H) or as a ketene (RCH═CO), respectively. Similarly, the signals at *m/z* 417.22 and 435.22 would be derived by neutral loss of the C18:0 chain as a fatty acid and as a ketene, respectively.

The positions (*sn*-1 versus *sn*-2) of the two fatty acyl chains on the glycerol backbone cannot be determined unequivocally by MS/MS analysis alone. However, Hsu and Turk reported a correlation between the abundances of the fatty acyl loss product ions and their positions on the glycerol backbone (*26*, *27*). In the MS/MS analysis of phosphatidylserine in the negative mode, they found that the product ions derived from the loss of the fatty acyl substituent at the *sn*-2 position were more abundant than those derived from loss at the *sn*-1 position (*26*, *27*). The expanded MS/MS spectrum (Figure 1B, inset) of the unknown at *m/z* 1026.78 shows that the ion at *m/z* 419.24 is more abundant than the one at *m/z* 417.22 and that the one at *m/z* 437.24 is more abundant than the one at *m/z* 435.22. We conclude that the C18:0 chain is attached predominantly to the *sn*-1 position and the C18:1 chain to the *sn*-2 position of the glycerol backbone (*26*, *27*).

The phosphatidic acid anion observed at *m/z* 701.49 (Figure 1B) was presumably derived during MS/MS from the $[M - H]^-$ ion at *m/z* 1026.73 (Figure 1B) by a neutral loss of 325.24 Da. The odd mass of the neutral loss fragment suggested that it contained an odd number of nitrogen atoms. The exact mass of the neutral loss, 325.261 Da, was determined by the mass difference between the accurately measured $[M - H]^-$ ion mass (1026.773) (Figure 1A) and the theoretical mass (701.512) of the C18:0/C18:1 phosphatidic acid anion. The exact mass of the neutral loss suggested an elemental composition of $C_{19}H_{35}NO_3$ (calculated exact mass 325.262 Da). This elemental composition, combined with the above MS/MS data, suggested *N*-palmitoylphosphatidylserine (C18:0/C18:1) as the structure that gives rise to the signal at *m/z* 1026.78 (Figure 1A,C). *N*-Acyl-PS has a net charge of −2, consistent with its elution from the DEAE-cellulose column together with cardiolipin.

Comparing Brain N-Acyl-PS with a Synthetic Standard by MS/MS and LC/MS. To confirm the proposed structure, a synthetic *N*-acyl-PS standard was prepared as described in the Experimental Procedures. As shown in Figure 2A, the synthetic *N*-acyl-PS, 1,2-dioleoyl-*sn*-glycerol-3-phosphoserine-*N*-nonadecanoate, has the formula $C_{61}H_{114}NO_{11}P$ and an exact mass of 1067.813 Da. The MS/MS spectrum of the $[M - H]^-$ ion of this standard, seen at *m/z* 1066.81 (Figure 2B), shows a fragmentation pattern that is very similar to that of the novel brain lipid (Figure 1B). The differences in the masses of the product ions are as predicted on the basis of the differences in the acyl chain compositions of the endogenous and the synthetic compounds.

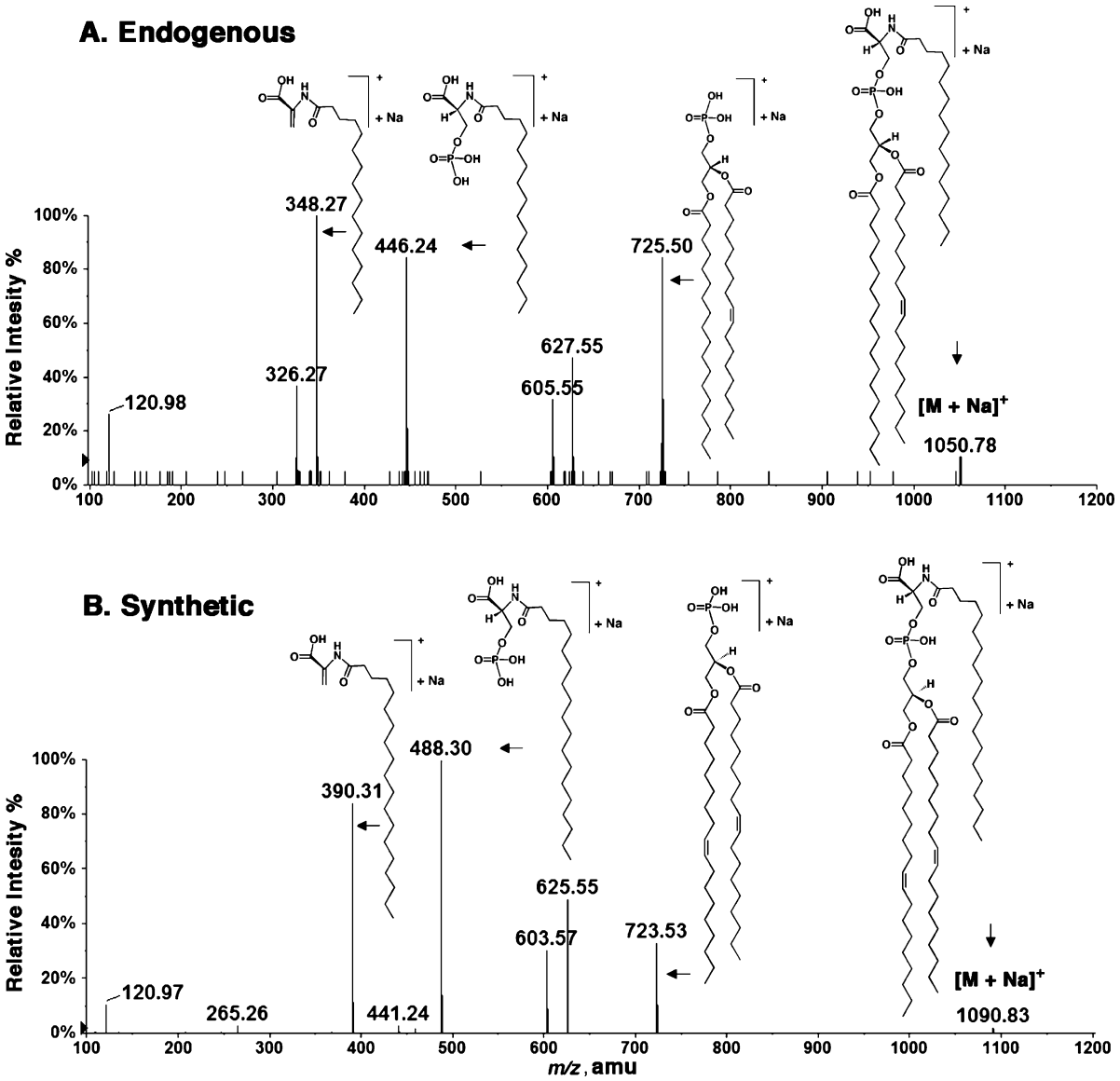

FIGURE 4: Comparison of the endogenous and synthetic *N*-acyl-PS molecules by MS/MS of their $[M + Na]^+$ ions: (A) MS/MS spectrum of the $[M + Na]^+$ ion at *m*/*z* 1050.78 (endogenous), (B) MS/MS spectrum of the $[M + Na]^+$ ion at *m*/*z* 1090.83 (synthetic). The proposed structures of the major product ions are shown.

MS/MS comparison of the endogenous material with the synthetic *N*-acyl-PS was also performed in the positive ion mode. The MS/MS analysis of the $[M + H]^+$ ion at *m*/*z* 1028.79 yielded prominent product ions (Figure 3A) at *m*/*z* 326.26 and 605.53, consistent with the expected fragmentation scheme for glycerophospholipids. The corresponding product ions for the synthetic standard were observed at *m*/*z* 368.33 and 603.55 (Figure 3B), consistent with its structure.

MS/MS analysis was also performed on the $[M + Na]^+$ ions of both compounds. Figure 4A shows the MS/MS spectrum of the sodium adduct of the endogenous *N*-acyl-PS $[M + Na]^+$ ion, which is seen at *m*/*z* 1050.78 (Figure 4A). In this case the major product ions are observed at *m*/*z* 120.98 for $[H_3PO_4 + Na]^+$, at *m*/*z* 348.27 for sodiated *N*-palmitoyldehydroalanine, at *m*/*z* 446.24 for the sodiated *N*-palmitoylphosphoserine, at *m*/*z* 605.55 for the protonated dehydrated diacylglycerol (C18:0/C18:1), at *m*/*z* 627.55 for the sodiated dehydrated diacylglycerol (C18:0/C18:1), and at *m*/*z* 725.50 for the sodiated phosphatidic acid adduct (C18:0/C18:1). All the expected, corresponding product ions were observed in the MS/MS spectrum of the $[M + Na]^+$ adduct of the synthetic *N*-acyl-PS standard (Figure 4B).

LC/MS comparison of the endogenous and synthetic *N*-acyl-PS was performed in the negative ion mode. Figure 5 shows the extracted ion chromatograms (EICs) of the $[M - H]^-$ ions derived from the endogenous *N*-palmitoyl-PS at *m*/*z* 1026.8 (Figure 5A) versus those derived from the synthetic standard at *m*/*z* 1066.8 (Figure 5B). The retention times of these two species during reversed-phase chromatography are consistent with their structural similarity. The synthetic *N*-acyl-PS, with its slightly longer acyl chains, emerges 1.14 min later than the endogenous *N*-palmitoyl-PS.

Presence of Additional N-Acyl-PS Molecular Species Including N-Arachidonoyl-PS. An expansion of the mass spectrum, shown in Figure 1A, in the range of *m*/*z* 980−1200 reveals the presence of a series of *N*-acyl-PS ions in addition to the prominent species at *m*/*z* 1026.80 (Figure 6A). When subjected to exact mass measurements and MS/MS analysis, these *N*-acyl-PS species were found to be complex

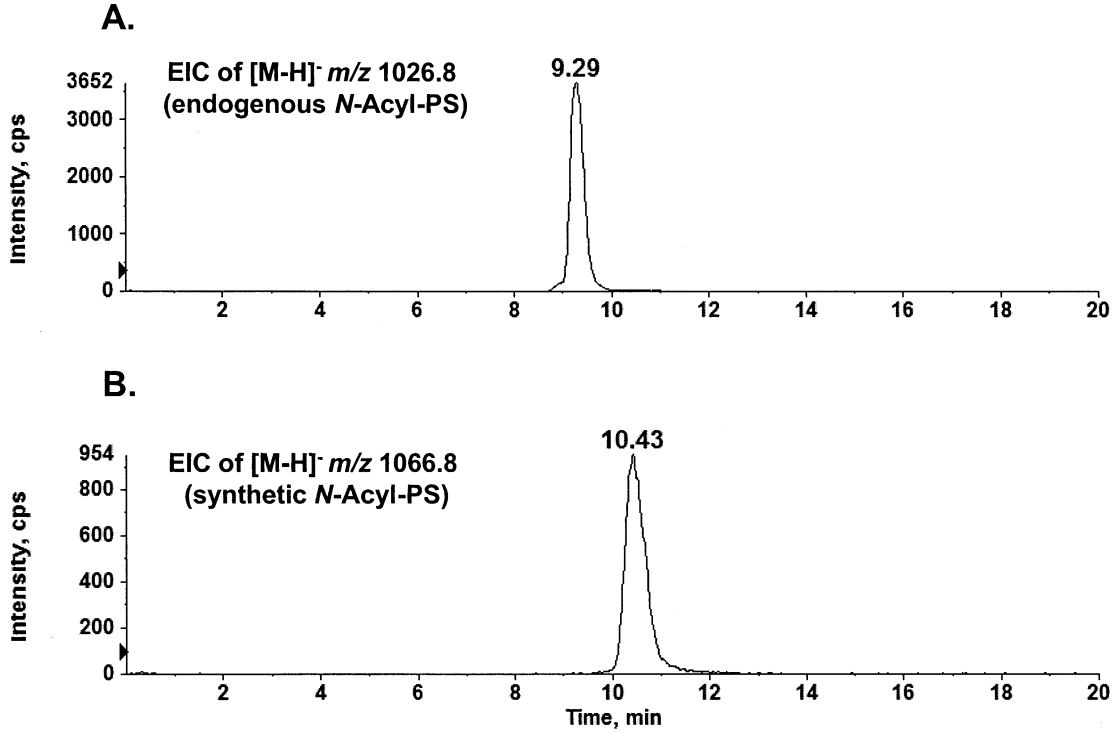

FIGURE 5: Comparison of endogenous and synthetic *N*-acyl-PS molecules by LC/MS in the negative ion mode: (A) EIC of the $[M - H]^-$ ion at *m*/*z* 1026.8 for the endogenous *N*-acyl-PS, (B) EIC of the $[M - H]^-$ ion at *m*/*z* 1066.8 for the synthetic *N*-acyl-PS.

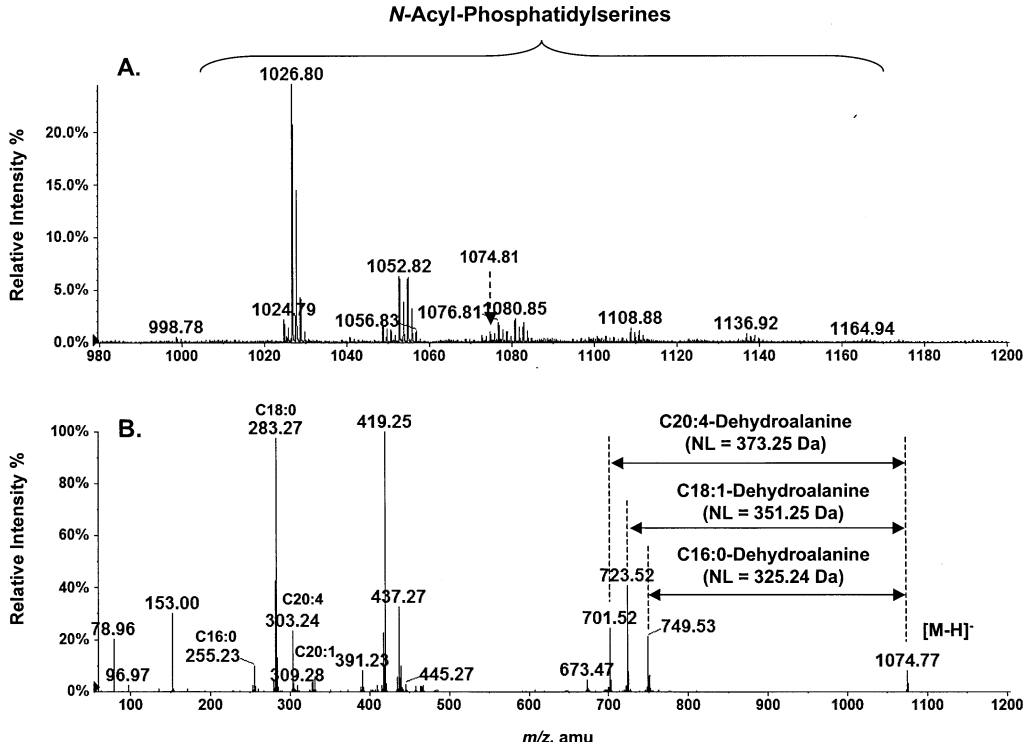

FIGURE 6: A family of *N*-acyl-PS molecular species in mouse brain. (A) Expanded negative ion mass spectrum (*m*/*z* 980−1200) from Figure 1A showing a family of putative *N*-acyl-PS $[M - H]^-$ ions. These *N*-acyl-PS species (see Table 1) were identified by the exact mass measurements and MS/MS analysis. (B) Complex *N*-acyl chain compositions, as revealed by MS/MS analysis of the peak at *m*/*z* 1074.77. The neutral losses in the MS/MS were used to identify the *N*-acyl chains: 373.25 Da for *N*-arachidonoyl-PS, 351.25 Da for *N*-oleoyl-PS, and 325.24 Da for *N*-palmitoyl-PS.

because of the heterogeneity of their *O*- and *N*-linked acyl chains. As illustrated in Figure 1B with the MS/MS of the ion at *m*/*z* 1026.80, the various *O*-linked fatty acyl groups could be assigned on the basis of the masses of the released fatty acid anions. The structures of *N*-linked acyl chains were deduced from the masses of the neutral losses yielding the phosphatidic acidic anions. The *N*-acyl-PS molecular species detected in this manner, together with their associated *N*-acyl chains, are listed in Table 1.

N-Arachidonoyl-PS was detected by MS/MS analysis of the ion at *m*/*z* 1074.77 (Figure 6B). The product ions at *m*/*z* 255.23, 281.25, 283.27, 303.24, and 309.28 are the anions

Table 1: Proposed *N*-Acyl-PS Molecular Species Detected in Mouse Brain[a]

$[M-H]^-$ (*m/z*)	NL	*N*-acyl chain	$[M-H]^-$ (*m/z*)	NL	*N*-acyl chain	$[M-H]^-$ (*m/z*)	NL	*N*-acyl chain
998.7	297	C14:0	1074.8	325	C16:0	1134.8	351	C18:1
	325	C16:0		351	C18:1		379	C20:1
1012.8	311	C15:0		373	C20:4		407	C22:1
	325	C16:0		401	C22:4		435	C24:1
	339	C17:0	1076.8	325	C16:0	1136.8	325	C16:0
	353	C18:0		351	C18:1		351	C18:1
1024.8	323	C16:1		353	C18:0		353	C18:0
	325	C16:0		375	C20:3		379	C20:1
	351	C18:1	1080.8	325	C16:0		381	C20:0
1026.8	325	C16:0		351	C18:1		407	C22:1
1038.8	311	C15:0		353	C18:0		435	C24:1
	325	C16:0		379	C20:1		437	C24:0
	337	C17:1	1102.8	325	C16:0	1138.8	325	C16:0
	339	C17:0		351	C18:1		353	C18:0
	351	C18:1		353	C18:0		381	C20:0
	353	C18:0		373	C20:4		409	C22:0
1040.8	311	C15:0		379	C20:1		437	C24:0
	325	C16:0		401	C22:4		465	C26:0
	339	C17:0	1108.8	325	C16:0	1164.8	379	C20:1
	353	C18:0		351	C18:1		381	C20:0
1048.8	325	C16:0		353	C18:0		407	C22:1
1050.8	325	C16:0		379	C20:1		409	C22:0
	351	C18:1		407	C22:1		435	C24:1
	377	C20:2		435	C24:1		437	C24:0
1052.8	325	C16:0	1122.8	325	C16:0		463	C26:1
	351	C18:1		351	C18:1		465	C26:0
	353	C18:0		353	C18:0	1166.8	409	C22:0
1054.8	325	C16:0		421	C23:1		437	C24:0
	353	C18:0	1124.8	325	C16:0		465	C26:0
1072.7	325	C16:0		353	C18:0			
	351	C18:1		395	C21:0			
	373	C20:4		423	C23:0			
	399	C22:5		437	C24:0			

[a] The numbers of carbon atoms and double bonds of the *N*-linked fatty acyl chains were deduced from the neutral losses observed in the negative ion MS/MS spectra of the indicated $[M-H]^-$ rounded to the nearest 0.1 amu. NL = neutral loss, rounded to the nearest integer; only the most prominent NL species are shown for each $[M-H]^-$. We cannot exclude the possibility that the putative odd-chain species actually represent *N*-acylated phosphatidylthreonines.

of C16:0, C18:1, C18:0, C20:4, and C20:1 fatty acids, respectively, indicating that these are the possible combinations of fatty acyl moieties esterified to the glycerol backbone. The sizes of the neutral loss fragments arising during collisional activation of the isobaric ions at *m/z* 1074.77 were used to identify the *N*-acyl chains: 325.24 Da for *N*-palmitoyl-PS, 351.25 Da for *N*-oleoyl-PS, and 373.25 Da for *N*-arachidonoyl-PS. As discussed below, *N*-arachidonoyl-PS might be a biosynthetic precursor of the recently discovered signaling lipid *N*-arachidonoylserine (*15*).

Identification and Mild Alkaline Hydrolysis of N-Acyl-PS from Pig Brain. Commercial pig brain lipids (Avanti) were fractionated on a 100 mg scale by chromatography on DEAE-cellulose as described above for mouse brain lipids. The compounds eluting with 120 mM ammonium acetate as the aqueous component were again enriched in various molecular species of *N*-acyl-PS (data not shown). To confirm their identity, the partially purified *N*-acyl-PS was subjected to *O*-deacylation in chloroform/methanol/0.38 M aqueous NaOH (1:2:0.8, v/v) for 60 min at room temperature (Scheme 1), yielding a series of *N*-acylated glycerophosphoserines (NAGPSs). Figure 7 shows the LC/MS analysis of the *O*-deacylated pig brain *N*-acyl-PS. The negative ion mass spectra acquired between 1 and 1.5 min of reversed-phase chromatography (Figure 7A) were consistent with the presence of a series of NAGPS molecules bearing C16:0, C18:1, C20:4, C24:1, or C26:1 fatty acyl chains. The NAGPS species containing arachidonate at *m/z* 544.263 was a minor, but nevertheless significant, component (Figure 7A, inset). The mass spectra acquired between 2 and 2.5 min of chromatography (Figure 7B) revealed NAGPSs, containing longer acyl chains (C26:1, C26:0, C28:1, or C30:1). About 30 different *N*-acyl groups (Table 2) were identified. Representative negative ion MS/MS spectra of NAGPS species, those bearing C16:0, C20:4, or C30:1 chains, are shown in Figure 8. All yielded the identical, expected product ions.

Table 2: Observed and Predicted Exact Masses of the $[M-H]^-$ Ions of the Mild Alkaline Hydrolysis Products of *N*-Acyl-PS from Porcine Brain[a]

	$[M-H]^-$			$[M-H]^-$	
NAGPS	obsd mass	exact mass	NAGPS	obsd mass	exact mass
C14:0	468.234	468.237	C22:4	574.308	574.315
C15:0	482.250	482.252	C22:3	576.321	576.331
C16:1	494.246	494.252	C22:1	578.338	578.346
C16:0	496.255	496.268	C22:0	580.349	580.362
C17:1	508.263	508.268	C23:1	592.361	592.362
C17:0	510.275	510.284	C24:1	606.368	606.378
C18:1	522.270	522.284	C24:0	608.390	608.393
C18:0	524.293	524.299	C25:1	620.398	620.393
C20:4	544.263	544.268	C25:0	622.397	622.409
C20:3	546.276	546.284	C26:1	634.400	634.409
C20:2	548.292	548.299	C26:0	636.421	636.425
C20:1	550.311	550.315	C27:1	648.425	648.425
C20:0	552.326	552.331	C28:1	662.439	662.440
C22:6	570.283	570.284	C28:0	664.447	664.456
C22:5	572.298	572.299	C30:1	690.464	690.472

[a] The structure of NAGPS (C16:0) is shown in Scheme 1. The apparent odd-chain species are minor components. We cannot exclude the possibility that they are actually *N*-acylated phosphatidylthreonines.

Estimation of the Levels of Pig Brain N-Acyl-PS by Liquid Chromatography and Multiple Reaction Monitoring. To estimate the level of the major brain *N*-acyl-PS, a known quantity of the synthetic *N*-acyl-PS standard was added to total porcine brain lipids (Avanti), followed by the determination of the ion signal ratio of the endogenous and the synthetic species. This was achieved by LC-coupled MRM on an ABI 4000 Q-Trap hybrid triple-quadrupole linear ion trap mass spectrometer. Figure 9 shows the LC−MRM chromatograms derived from the most abundant endogenous *N*-palmitoyl-PS (C18:0/C18:1) species (the MRM pair of 1026.8/701.6) present in 1 μg of total porcine brain lipid versus 1 ng of the synthetic *N*-acyl-PS standard (the MRM pair of 1066.8/699.6). Assuming that the signal responses are very similar for these two closely related lipids (Figures 1C and 2A), the peak area ratio of 0.4 indicates that there is about 0.4 ng (or 0.04% by weight) of the most abundant endogenous *N*-acyl-PS in 1 μg of porcine brain lipids. Since the most abundant *N*-acyl-PS species accounts for about 40% of all the *N*-acyl-PS species, we estimate that the combined *N*-acyl-PS species make up about 0.1% of the porcine brain lipid. Although our synthetic standard is not an isotopically labeled analogue, its structure is nevertheless very close to that of the endogenous species (Figures 1 and 2) and thus should have similar ionization efficiency.

Detection of N-Acyl-PS in RAW264.7 and Yeast Cells. By carrying out lipid prefractionation in conjunction with high-

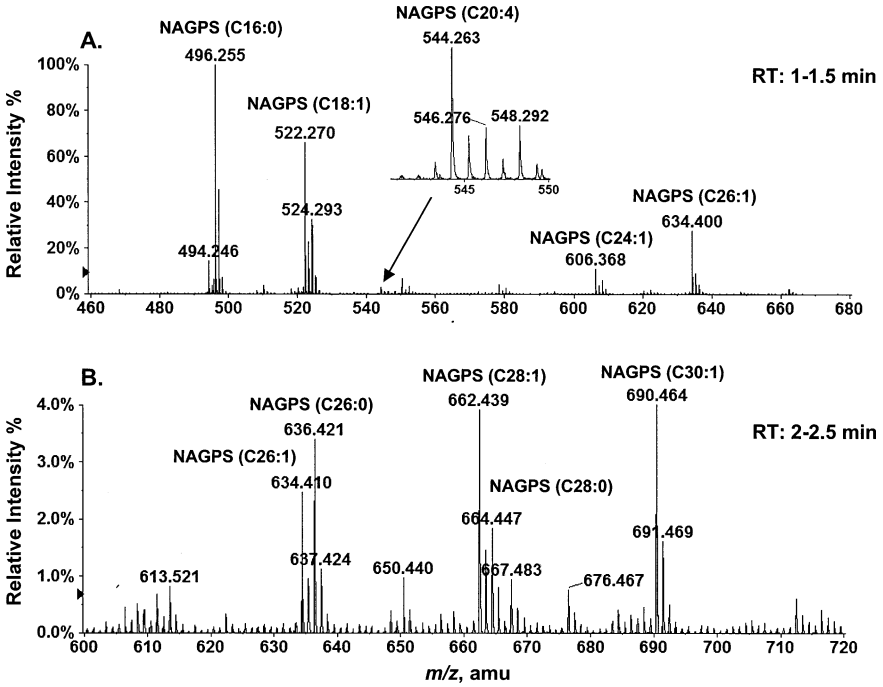

FIGURE 7: LC/MS detection of *N*-acylglycerophosphoserines produced by mild alkaline hydrolysis of porcine brain *N*-acyl-PS. (A) Mass spectrum (averaged from the spectra acquired during 1−1.5 min) of the NAGPSs with acyl chains of C16:0, C18:1, C24:3, and C26:3. The inset shows the magnified peak near *m*/*z* 544 for NAGPS (C20:4), providing additional evidence for the existence of *N*-arachidonoyl-PS. (B) Mass spectrum (averaged from the spectra acquired during 2−2.5 min) of the NAGPS chromatography with very long acyl chains (C26:3, 26:2, C28:1, and C30:1). The structures of NAGPS (C16:0), NAGPS (C20:4), and NAGPS (C30:1) were confirmed by both MS/MS (Figure 8) and accurate mass measurements (Table 2).

Scheme 1: Mild Alkaline Hydrolysis of *N*-Acyl-PS[a]

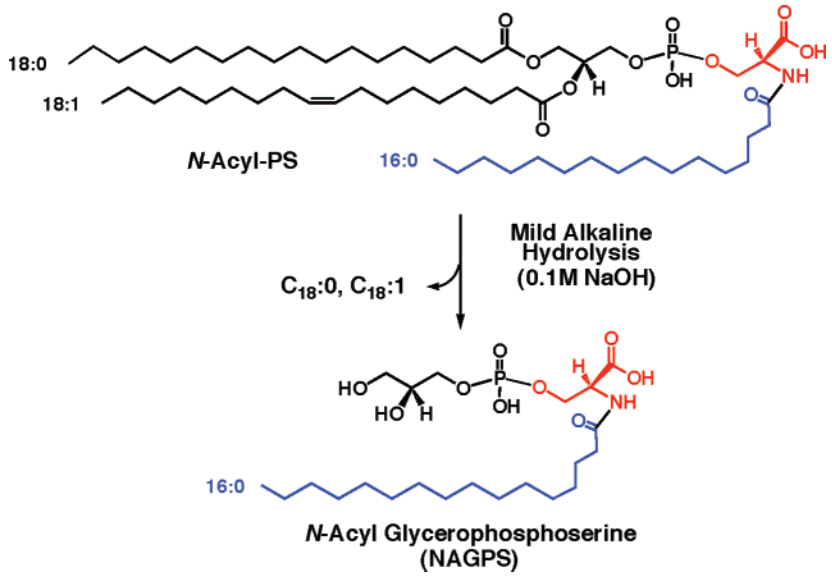

[a] This *N*-acyl-PS structure is the most abundant brain *N*-acyl-PS molecular species.

resolution MS analysis, we also detected low levels of *N*-acyl-PS in the mouse RAW264.7 macrophage cells and yeast. Figure 10A is the negative ion ESI mass spectrum of the 120 mM ammonium acetate fraction of DEAE-cellulose-fractionated RAW264.7 cell lipids. The signal intensities of the *N*-acyl-PS ions (Figure 10B) are 2 orders of magnitude lower than those from brain (compare Figures 1 and 10). Improved detection of these species was made possible by using LC/MS (data not shown). The major ions arising from the *N*-acyl-PS molecular species of RAW cells (*m*/*z* 998.73, 1024.75, 1026.77, 1052.76 in Figure 10B) are the same as those found in mouse brain (Figure 6A). The relatively high levels of *N*-acyl-PS species in the brain suggest that they may play special roles in the central nervous system.

N-Acyl-PS molecular species were also detected in yeast total lipid extracts (data not shown) using LC−MRM on an ABI 4000 Q-Trap hybrid triple-quadrupole linear ion trap mass spectrometer. The major *N*-acyl-PS species detected are *N*-palmitoyl-PS (C16:0/C18:1) (MRM 998.8/673.5), *N*-myristoyl-PS (C16:0/C18:1) (MRM 970.7/673.5), and *N*-stearoyl-PS (C16:0/C18:1) (MRM 1026.8/673.5). The presence of *N*-acyl-PS species in yeast should facilitate enzymatic and genetic studies of their biosynthesis.

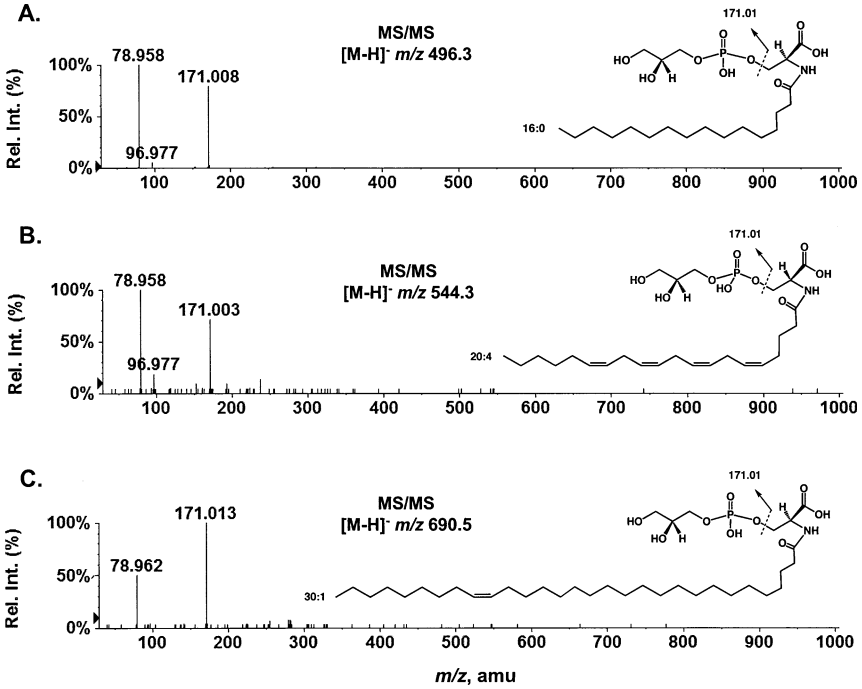

FIGURE 8: MS/MS analysis of three NAGPSs produced by mild alkaline hydrolysis of *N*-acyl-PS: (A) MS/MS of the $[M - H]^-$ ion at *m*/*z* 496.3 for NAGPS (C16:0), (B) MS/MS of the $[M - H]^-$ ion at *m*/*z* 544.3 for NAGPS (C20:4), and (C) MS/MS of the $[M - H]^-$ ion at *m*/*z* 690.5 for NAGPS (C30:1). The positions of the double bonds were not determined by MS/MS, but were inferred from the literature (*6*, *10*).

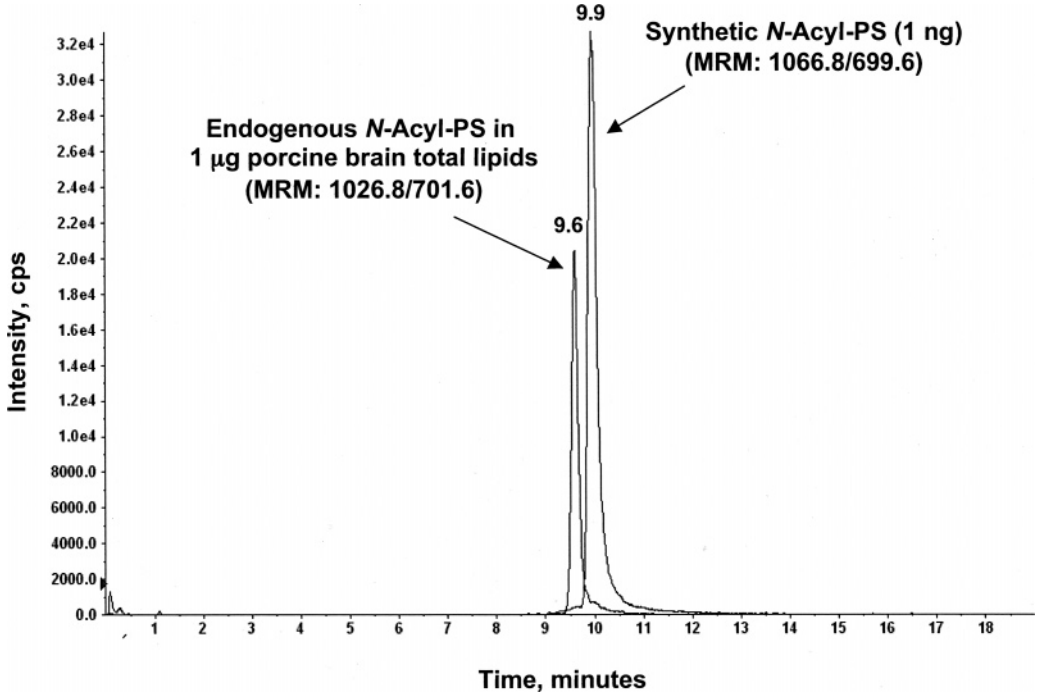

FIGURE 9: Quantification of the most abundant porcine brain *N*-acyl-PS species by LC−MRM. The two LC−MRM chromatograms refer to the most abundant endogenous *N*-acyl-PS species (MW 1027.8) present in 1 μg of porcine brain total lipid (MRM pair of 1026.8/701.6) versus 1 ng of added synthetic *N*-acyl-PS standard (MRM pair of 1066.8/699.6).

DISCUSSION

The question of whether *N*-acyl-PS is a naturally occurring phospholipid has remained unanswered for over 35 years. Nelson first reported the presence of *N*-acyl-PS in sheep erythrocytes (*28*), but his structural analysis was based only on infrared spectroscopy, thin-layer chromatography, and elemental analysis (*28*). In 1982, Donohue et al. reported *N*-acyl-PS as a major phospholipid in *R. sphaeroides* (*13*). However, this claim was challenged by Schmid et al., who demonstrated conclusively that the material isolated by Donohue et al. was actually phosphatidyl-Tris, unexpectedly generated by microbial incorporation of exogenous Tris buffer into phospholipid (*14*).

We have now demonstrated the presence of a family of *N*-acyl-PS molecules in mouse brain, pig brain, RAW macrophage tumor cells, and yeast using high-resolution

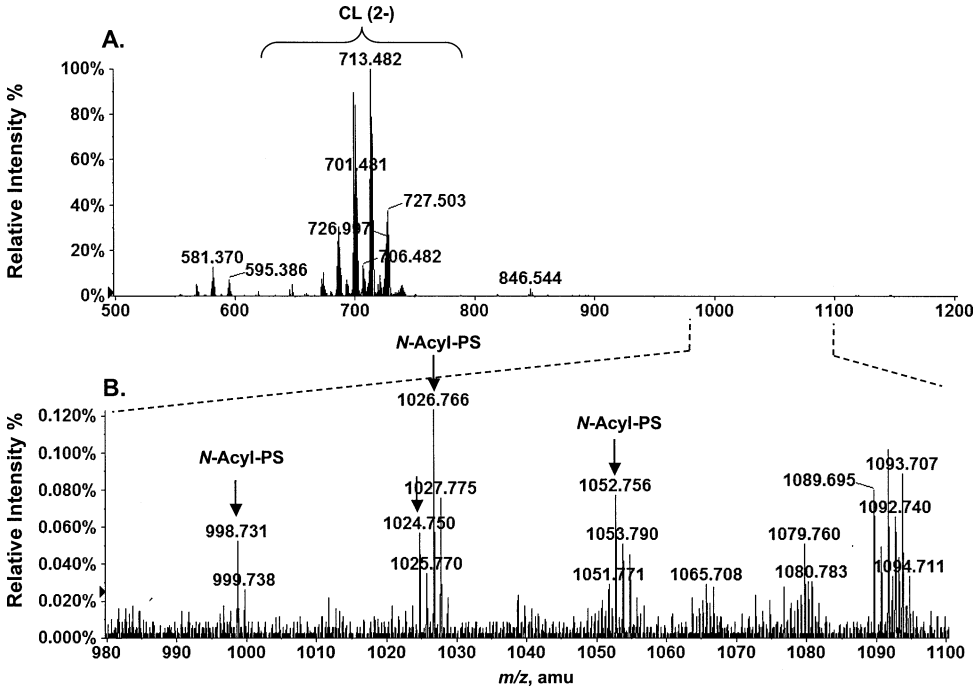

FIGURE 10: Detection of *N*-acyl-PS molecular species in RAW cells: (A) negative ion ESI mass spectrum of phospholipid species eluting with 120 mM ammonium acetate from a DEAE-cellulose column, (B) expanded mass spectrum (*m*/*z* 980−1100) showing the $[M - H]^-$ ions of *N*-acyl-PS species present in RAW cells.

tandem ESI-MS. Our initial identification of *N*-acyl-PS was facilitated by chromatographic enrichment of dianionic phospholipids on a DEAE-cellulose column (Figure 1). The structural elucidation involved accurate mass measurements, tandem MS, and comparison to a synthetic standard. Brain *N*-acyl-PS consists of a large number of molecular species, given the presence of at least 30 different *N*-linked acyl chains (Tables 1 and 2). *N*-Palmitoyl-PS is the major component, but there are many additional molecular species, including *N*-arachidonyl-PS. In aggregate, we estimate that these *N*-acyl-PS molecules constitute ~0.1% of the total brain lipid or about 0.001% of the total RAW cell lipid, whereas phosphatidylserine typically makes up ~7% of the RAW phospholipid (*4*).

The unequivocal identification of a novel collection of *N*-acyl-PS molecular species in mammalian cells and yeast will enable investigations into their biosynthesis, turnover, and biological functions. *N*-Acyl-PS is structurally similar to *N*-acyl-PE, which has recently received considerable attention (*16*−*18*). First discovered as a novel lipid that accumulates in myocardial infarcts (*29*), *N*-acyl-PEs are formed by an enzyme that transfers the *sn*-1-acyl chain of a glycerophospholipid to the primary amine of PE in a calcium-dependent manner (*30*−*32*). The identity of the structural gene(s) encoding the relevant Ca^{2+}-dependent transacylase is unknown (*16*). Importantly, the *N*-acyl-PEs are biosynthetic precursors of a class of lipophilic signaling molecules, the *N*-acyl ethanolamines (*16*, *33*), which include the endocannabinoid anandamide (*N*-arachidonoylethanolamine) (*34*, *35*), the anti-inflammatory agent *N*-palmitoylethanolamine (*36*), the satiety-inducing factor *N*-oleoylethanolamine (*37*), and the proapoptotic lipid *N*-steroylethanolamine (*38*) (*26*). Given the *N*-acyl-PE precedent, we speculate that some of the *N*-acyl-PS molecular species shown in Table 1 might be hydrolyzed to produce the corresponding *N*-acylserines. Recently, the novel signaling lipid *N*-arachidonoyl-L-serine was isolated from bovine brain in trace amounts (*15*). The biological and physiological functions of *N*-arachidonoyl-L-serine include vasodilation of rat isolated mesenteric arteries and abdominal aorta and the suppression of LPS-induced TNF-α production by RAW macrophage tumor cells (*15*).

We envisage two possibilities for the formation and metabolism of *N*-acyl-PS. In the first scenario, *N*-acyl-PS could arise, as noted above, by a transacylation reaction, similar to the one that generates *N*-acyl-PE (Scheme 2). The same enzyme might generate *N*-acyl-PS, but the possibility of a distinct transacylase cannot be excluded. According to Scheme 2, in vitro incubation of [^{32}P]PS with an appropriate phospholipid cosubstrate, such as PC (C16:0/C18:1), should result in the formation of *N*-palmitoyl-PS, the major *N*-acyl-PS species seen in brain and RAW cells (Figures 1 and 10). To demonstrate the absolute dependence of *N*-palmitoyl-PS formation on the presence of the added palmitoyl donor PC (C16:0/C18:1), the transacylase may have to be partially purified to remove endogenous phospholipids. The turnover of *N*-acyl-PS by a phosholipase D (Scheme 2) is proposed in analogy to *N*-acyl-PE turnover (*18*). This is the most obvious mechanism for the formation of *N*-acylserine. However, *N*-acyl-PS might first be deacylated by a phospholipase A (*33*, *39*) and then converted to *N*-acylserine by a phosphodiesterase (not shown).

An alternative mechanism for the formation of *N*-acyl-PS (Scheme 3) involves the formation of *N*-acylserine from acyl-coenzyme A and serine, followed by headgroup exchange with phosphatidylcholine (or phosphatidylethanolamine) to generate *N*-acyl-PS. Exchange reactions of this type are the route by which phosphatidylserine is synthesized in animal cells (*40*). Two distinct serine exchange enzymes have been identified. One is specific for phosphatidylcholine and the

Scheme 2: Proposed Hypothetical Pathway for the Biosynthesis of *N*-Acyl-PS and Its Conversion to *N*-Acylserine[a]

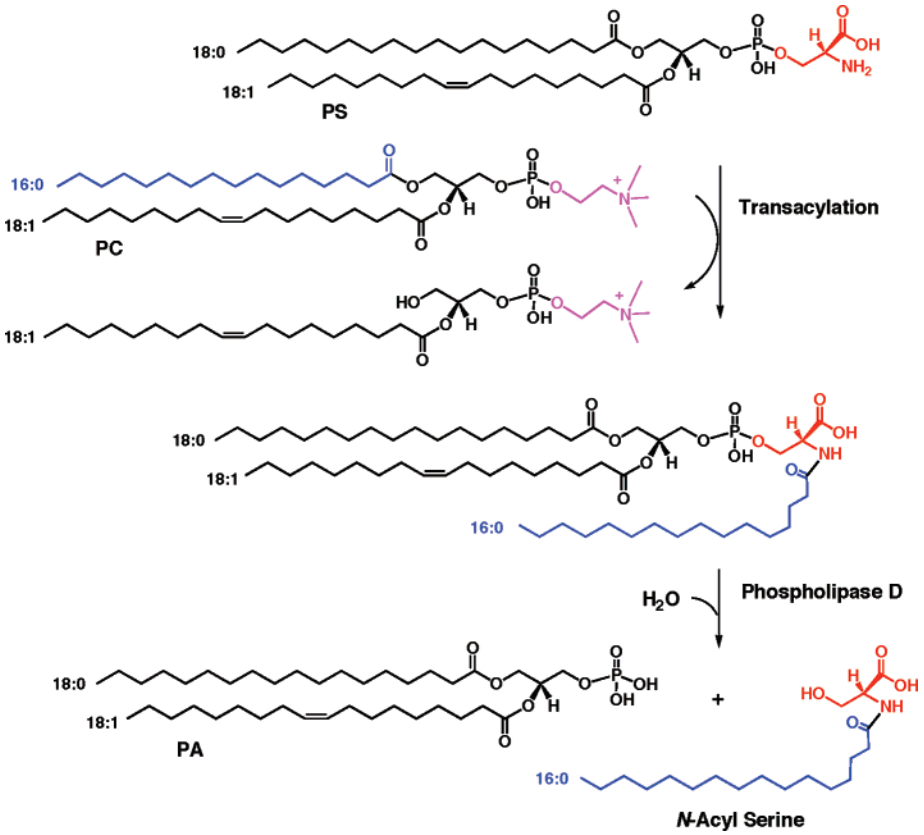

[a] These reactions are analogous to those involved in the formation of *N*-acyl-PE and anandamide. Abbreviations: PC, phosphatidylcholine; PS, phosphatidylserine; PA, phosphatidic acid. Presumably other glycerophospholipids can substitute as acyl donors. The predominance of the *N*-palmitoyl moiety in the *N*-acyl-PS series suggests that the *N*-acyl chain arises mainly from the *sn*-1 position of donor glycerophospholipids.

Scheme 3: An Alternative Hypothetical Pathway for the Formation of *N*-Acyl-PS[a]

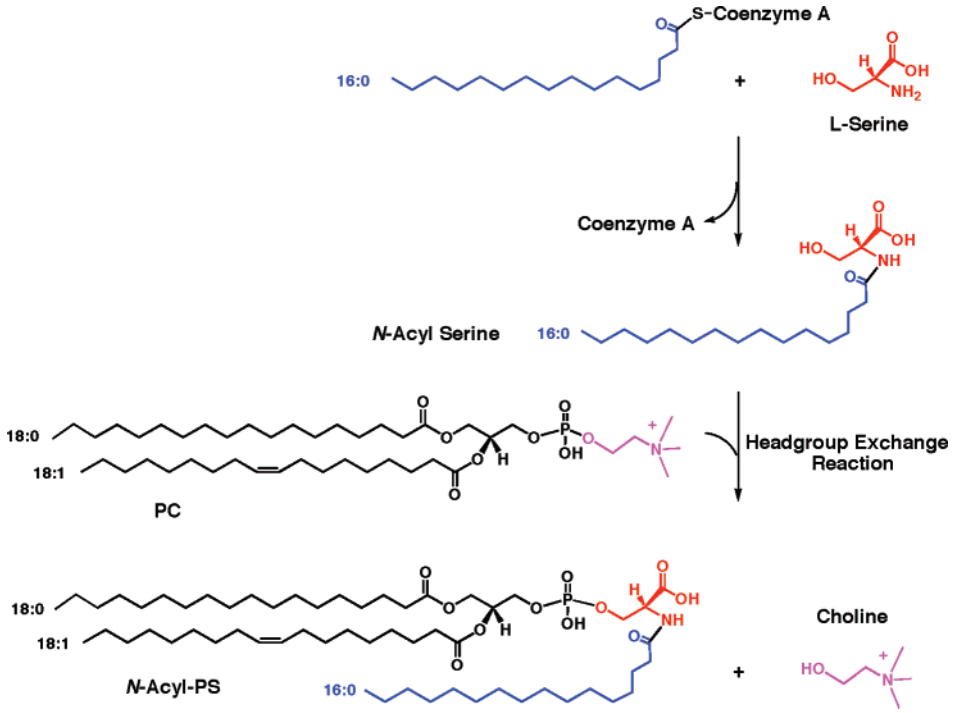

[a] In animal cells phosphatidylserine is generated by a headgroup exchange reaction involving phosphatidylcholine (or phosphatidylethanolamine) and free serine (*40*). In principle, *N*-acylserine could substitute for serine. PC = phosphatidylcholine.

other for phosphatidylethanolamine (not shown) (*40*). These reactions are also calcium ion dependent. The relevant structural genes have been cloned and the enzymatic activities characterized (*41*), but *N*-acylserine was not tested as a

phosphatidyl group acceptor (*41*). Studies of the biosynthesis and degradation of *N*-acyl-PS are currently under way in our laboratory to distinguish between these possibilities.

ACKNOWLEDGMENT

We thank Dr. Teresa Garrett, Mr. Ramesh Ghattamaneni, and Mr. Reza Kordestani for their expertise and assistance in RAW cell culture and lipid fractionation and Dr. Robert Murphy for sharing the conditions of liquid chromatography for lipid analysis.

REFERENCES

1. Fahy, E., Subramaniam, S., Brown, H. A., Glass, C. K., Merrill, A. H., Jr., Murphy, R. C., Raetz, C. R. H., Russell, D. W., Seyama, Y., Shaw, W., Shimizu, T., Spener, F., van Meer, G., VanNieuwenhze, M. S., White, S. H., Witztum, J. L., and Dennis, E. A. (2005) A comprehensive classification system for lipids, *J. Lipid Res. 46*, 839−862.
2. Dennis, E. A., Brown, H. A., Deems, R., Glass, C. K., Merrill, A. H., Murphy, R. C., Raetz, C. R. H., Shaw, W., Subramaniam, S., Russell, D. W., van Nieuwenhze, M., White, S. H., Witztum, J. L., and Wooley, J. (2005) The LIPID MAPS approach to lipidomics, in *Functional Lipidomics* (Feng, L., and Prestwich, G. D., Eds.) pp 1−15, CRC Press/Taylor and Francis Group, Boca Raton, FL.
3. Raetz, C. R. H. (1986) Molecular genetics of membrane phospholipid synthesis, *Annu. Rev. Genet. 20*, 253−295.
4. Zoeller, R. A., Wightman, P. D., Anderson, M. S., and Raetz, C. R. H. (1987) Accumulation of lysophosphatidylinositol in RAW 264.7 macrophage tumor cells stimulated by lipid A precursors, *J. Biol. Chem. 262*, 17212−17220.
5. Riley, M., Abe, T., Arnaud, M. B., Berlyn, M. K., Blattner, F. R., Chaudhuri, R. R., Glasner, J. D., Horiuchi, T., Keseler, I. M., Kosuge, T., Mori, H., Perna, N. T., Plunkett, G., III, Rudd, K. E., Serres, M. H., Thomas, G. H., Thomson, N. R., Wishart, D., and Wanner, B. L. (2006) *Escherichia coli* K-12: a cooperatively developed annotation snapshot−2005, *Nucleic Acids Res. 34*, 1−9.
6. Murphy, R. C., Fiedler, J., and Hevko, J. (2001) Analysis of nonvolatile lipids by mass spectrometry, *Chem. Rev. 101*, 479−526.
7. Han, X., Yang, J., Cheng, H., Ye, H., and Gross, R. W. (2004) Toward fingerprinting cellular lipidomes directly from biological samples by two-dimensional electrospray ionization mass spectrometry, *Anal. Biochem. 330*, 317−331.
8. Fenn, J. B., Mann, M., Meng, C. K., Wong, S. F., and Whitehouse, C. M. (1989) Electrospray ionization for mass spectrometry of large biomolecules, *Science 246*, 64−71.
9. Karas, M., and Hillenkamp, F. (1988) Laser desorption ionization of proteins with molecular masses exceeding 10,000 daltons, *Anal. Chem. 60*, 2299−2301.
10. Pulfer, M., and Murphy, R. C. (2003) Electrospray mass spectrometry of phospholipids, *Mass. Spectrom. Rev. 22*, 332−364.
11. Ivanova, P. T., Cerda, B. A., Horn, D. M., Cohen, J. S., McLafferty, F. W., and Brown, H. A. (2001) Electrospray ionization mass spectrometry analysis of changes in phospholipids in RBL-2H3 mastocytoma cells during degranulation, *Proc. Natl. Acad. Sci. U.S.A. 98*, 7152−7157.
12. Guan, Z., Breazeale, S. D., and Raetz, C. R. H. (2005) Extraction and identification by mass spectrometry of undecaprenyl diphosphate-MurNAc-pentapeptide-GlcNAc from *Escherichia coli*, *Anal. Biochem. 345*, 336−339.
13. Donohue, T. J., Cain, B. D., and Kaplan, S. (1982) Purification and characterization of an N-acylphosphatidylserine from *Rhodopseudomonas sphaeroides*, *Biochemistry 21*, 2765−2773.
14. Schmid, P. C., Kumar, V. V., Weis, B. K., and Schmid, H. H. O. (1991) Phosphatidyl-Tris rather than N-acylphosphatidylserine is synthesized by *Rhodopseudomonas sphaeroides* grown in Tris-containing media, *Biochemistry 30*, 1746−1751.
15. Milman, G., Maor, Y., Abu-Lafi, S., Horowitz, M., Gallily, R., Batkai, S., Mo, F. M., Offertaler, L., Pacher, P., Kunos, G., and Mechoulam, R. (2006) *N*-arachidonoyl L-serine, an endocannabinoid-like brain constituent with vasodilatory properties, *Proc. Natl. Acad. Sci. U.S.A. 103*, 2428−2433.
16. McKinney, M. K., and Cravatt, B. F. (2005) Structure and function of fatty acid amide hydrolase, *Annu. Rev. Biochem. 74*, 411−432.
17. Cravatt, B. F., and Lichtman, A. H. (2004) The endogenous cannabinoid system and its role in nociceptive behavior, *J. Neurobiol. 61*, 149−160.
18. Leung, D., Saghatelian, A., Simon, G. M., and Cravatt, B. F. (2006) Inactivation of N-acyl phosphatidylethanolamine phospholipase D reveals multiple mechanisms for the biosynthesis of endocannabinoids, *Biochemistry 45*, 4720−4726.
19. Wang, C., Wilson, W. A., Moore, S. D., Mace, B. E., Maeda, N., Schmechel, D. E., and Sullivan, P. M. (2005) Human apoE4-targeted replacement mice display synaptic deficits in the absence of neuropathology, *Neurobiol. Dis. 18*, 390−398.
20. Dulbecco, R., and Vogt, M. (1954) Plaque formation and isolation of pure lines with poliomyelitis viruses, *J. Exp. Med. 99*, 167−182.
21. Bligh, E. G., and Dyer, J. J. (1959) A rapid method of total lipid extraction and purification, *Can. J. Biochem. Physiol. 37*, 911−917.
22. Raetz, C. R. H., and Kennedy, E. P. (1973) Function of cytidine diphosphate-diglyceride and deoxycytidine diphosphate-diglyceride in the biogenesis of membrane lipids in *Escherichia coli*, *J. Biol. Chem. 248*, 1098−1105.
23. Zhou, Z., Lin, S., Cotter, R. J., and Raetz, C. R. H. (1999) Lipid A modifications characteristic of *Salmonella typhimurium* are induced by NH_4VO_3 in *Escherichia coli* K12. Detection of 4-amino-4-deoxy- L-arabinose, phosphoethanolamine and palmitate, *J. Biol. Chem. 274*, 18503−18514.
24. Raetz, C. R. H., Garrett, T. A., Reynolds, C. M., Shaw, W. A., Moore, J. D., Smith, D. C., Jr., Ribeiro, A. A., Murphy, R. C., Ulevitch, R. J., Fearns, C., Reichart, D., Glass, C. K., Benner, C., Subramaniam, S., Harkewicz, R., Bowers-Gentry, R. C., Buczynski, M. W., Cooper, J. A., Deems, R. A., and Dennis, E. A. (2006) $(Kdo)_2$-lipid A of *Escherichia coli*, a defined endotoxin that activates macrophages via TLR-4, *J. Lipid Res. 47*, 1097−1111.
25. Radika, K., and Raetz, C. R. H. (1988) Purification and properties of lipid A disaccharide synthase of *Escherichia coli*, *J. Biol. Chem. 263*, 14859−14867.
26. Hsu, F. F., and Turk, J. (2000) Charge-remote and charge-driven fragmentation processes in diacyl glycerophosphoethanolamine upon low-energy collisional activation: a mechanistic proposal, *J. Am. Soc. Mass Spectrom. 11*, 892−899.
27. Hsu, F. F., and Turk, J. (2005) Studies on phosphatidylserine by tandem quadrupole and multiple stage quadrupole ion-trap mass spectrometry with electrospray ionization: structural characterization and the fragmentation processes, *J. Am. Soc. Mass Spectrom. 16*, 1510−1522.
28. Nelson, G. J. (1970) Studies on the lipids of sheep red blood cells. IV. The identification of a new phospholipid. N-acyl phosphatidyl serine, *Biochem. Biophys. Res. Commun. 38*, 261−265.
29. Epps, D. E., Natarajan, V., Schmid, P. C., and Schmid, H. O. (1980) Accumulation of N-acylethanolamine glycerophospholipids in infarcted myocardium, *Biochim. Biophys. Acta 618*, 420−430.
30. Natarajan, V., Reddy, P. V., Schmid, P. C., and Schmid, H. H. (1982) N-Acylation of ethanolamine phospholipids in canine myocardium, *Biochim. Biophys. Acta 712*, 342−355.
31. Reddy, P. V., Natarajan, V., Schmid, P. C., and Schmid, H. H. (1983) N-Acylation of dog heart ethanolamine phospholipids by transacylase activity, *Biochim. Biophys. Acta 750*, 472−480.
32. Natarajan, V., Schmid, P. C., Reddy, P. V., Zuzarte-Augustin, M. L., and Schmid, H. H. O. (1983) Biosynthesis of N-acylethanolamine phospholipids by dog brain preparations, *J. Neurochem. 41*, 1303−1312.
33. Simon, G. M., and Cravatt, B. F. (2006) Endocannabinoid biosynthesis proceeding through glycerophospho-N-acyl ethanolamine and a role for alpha/beta-hydrolase 4 in this pathway, *J. Biol. Chem. 281*, 26465−26472.
34. Devane, W. A., Hanus, L., Breuer, A., Pertwee, R. G., Stevenson, L. A., Griffin, G., Gibson, D., Mandelbaum, A., Etinger, A., and Mechoulam, R. (1992) Isolation and structure of a brain constituent that binds to the cannabinoid receptor, *Science 258*, 1946−1949.
35. Calignano, A., La Rana, G., Giuffrida, A., and Piomelli, D. (1998) Control of pain initiation by endogenous cannabinoids, *Nature 394*, 277−281.
36. Lambert, D. M., Vandevoorde, S., Jonsson, K. O., and Fowler, C. J. (2002) The palmitoylethanolamide family: a new class of anti-inflammatory agents?, *Curr. Med. Chem. 9*, 663−674.

37. Di Marzo, V., Goparaju, S. K., Wang, L., Liu, J., Batkai, S., Jarai, Z., Fezza, F., Miura, G. I., Palmiter, R. D., Sugiura, T., and Kunos, G. (2001) Leptin-regulated endocannabinoids are involved in maintaining food intake, *Nature 410*, 822−825.
38. Maccarrone, M., Pauselli, R., Di Rienzo, M., and Finazzi-Agro, A. (2002) Binding, degradation and apoptotic activity of stearoylethanolamide in rat C6 glioma cells, *Biochem. J. 366*, 137−144.
39. Sun, Y. X., Tsuboi, K., Okamoto, Y., Tonai, T., Murakami, M., Kudo, I., and Ueda, N. (2004) Biosynthesis of anandamide and N-palmitoylethanolamine by sequential actions of phospholipase A2 and lysophospholipase D, *Biochem. J. 380*, 749−756.
40. Kuge, O., and Nishijima, M. (1997) Phosphatidylserine synthase I and II of mammalian cells, *Biochim. Biophys. Acta 1348*, 151−156.
41. Stone, S. J., and Vance, J. E. (1999) Cloning and expression of murine liver phosphatidylserine synthase (PSS)-2: differential regulation of phospholipid metabolism by PSS1 and PSS2, *Biochem. J. 342 (Pt 1)*, 57−64.

BI701907G